Libertas Academica
FREEDOM TO RESEARCH

REVIEW

Measuring Restriction Sizes Using Diffusion Weighted Magnetic Resonance Imaging: A Review

Melanie Martin

Department of Physics, University of Winnipeg and Department of Radiology, University of Manitoba.
Corresponding author email: m.martin@uwinnipeg.ca

Abstract: This article reviews a new concept in magnetic resonance as applied to cellular and biological systems. Diffusion weighted magnetic resonance imaging can be used to infer information about restriction sizes of samples being measured. The measurements rely on the apparent diffusion coefficient changing with diffusion times as measurements move from restricted to free diffusion regimes. Pulsed gradient spin echo (PGSE) measurements are limited in the ability to shorten diffusion times and thus are limited in restriction sizes which can be probed. Oscillating gradient spin echo (OGSE) measurements could provide shorter diffusion times so smaller restriction sizes could be probed.

Keywords: magnetic resonance imaging, nuclear magnetic resonance, diffusion, axon diameter, restricted diffusion, porous materials, central nervous system, oscillating gradients, diffusion-time

Introduction

This short invited article reviews diffusion techniques used to infer sizes of structures in samples that lead to restricted diffusion. It briefly explains the time dependence of the MRI-measured apparent diffusion coefficient. Then it explains how the time dependence is used to infer sizes of structures, such as axon diameters, in the sample. It then discusses the limitations of current methods inferring small sizes and briefly explains one possible alternative to overcome these limitations.

Diffusion

Molecules in a liquid undergo diffusion. Their mean square displacement depends on the diffusion time, Δ, as described by Einstein's relation $<r^2> = 2D\Delta$ (in one dimension) where D is the diffusion coefficient.[1] Molecules diffusing in a uniform medium with no barriers experience unrestricted diffusion. In non-uniform media (eg, porous samples and cellular tissues) barriers restrict molecular displacements so that the diffusion depends on the time scale of the study and the permeability of the barriers. Assuming Einstein's relation, $<r^2>$ during the time Δ can be used to find an apparent diffusion coefficient (ADC) that is less than D because of restrictions or hindrances to motion. Understanding the influence of the restrictions or hindrances on the ADC gives information about the geometry of the boundaries of the surrounding medium which, for MRI, could be tissues, rocks, concrete, cement, polymers, gases, etc.[2]

As an example, the ADC in a simple system consisting of molecules with diffusion coefficient D that are entirely restricted to a single pore of diameter a will depend on Δ. For $\Delta \ll a^2/(2D)$, the diffusion will appear almost unrestricted. For $\Delta \gg a^2/(2D)$, all molecules, regardless of their starting position, will be found anywhere in the pore.[3] Measurements as a function of Δ thus provide information about the structure in which the molecules are diffusing. Specifically, there will be a change in the ADC when measuring through the time $\Delta = a^2/(2D)$ which can be used to determine the pore size.

Traditional MR measurements of the ADC in different samples use the Pulsed Gradient Spin Echo (PGSE) sequence,[4] see Figure 1. After excitation, a magnetic field gradient pulse is applied to the sample for a short time. This causes the spins to obtain a
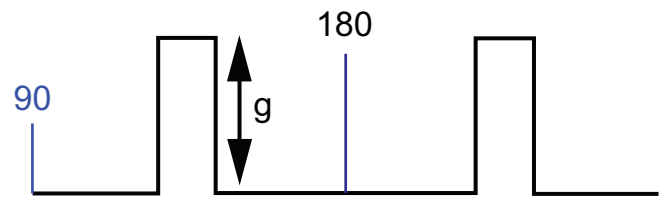
Figure 1. Pulsed gradient spin echo (PGSE) sequence. The basic PGSE sequence consists of two RF pulses, shown in blue, and two gradient pulses, shown in black. The diffusion time, Δ, is the time from the start of the first gradient pulse to the start of the second gradient pulse.

phase based on their position at the time of the pulse. A π RF pulse is then applied to the system which reverses the phase of the spins. Another identical gradient pulse is applied to the sample which changes the phase of the spins based on their position at the time of the second pulse (Δ). If no diffusion has occurred, the phase acquired from the second pulse will be equal and opposite to the phase of the spin just before the pulse, resulting in a net phase of zero. If diffusion occurs, the mean squared phase of all spins will be nonzero and cause a loss in MR signal which can be used to calculate the ADC.[4]

Alternatively, Callaghan proposed q-space imaging using PGSE with short gradient pulses to measure the conditional probability, $P(r'—r, \Delta)$, that a spin initially at r has migrated to r' over the time Δ. By measuring the signal as a function of gradient strength, one can calculate the probability distribution of displacements of spins.[5] Using this probability distribution, one can infer from MR images tissue geometric information, such as axon diameter distributions and axonal and cellular volume fractions or densities.[5–9] It is difficult, however, to find P in white matter because of the variability of axon diameter.[2]

In vivo measurements using echo planar imaging (EPI) sequences are used to acquire images more rapidly.[2] This allows full diffusion tensor imaging (DTI) in vivo although the resolution is often not as good as standard imaging sequences.[10] Perfusion can also be measured using MRI and the effects of perfusion on diffusion measurements must be taken into account.[11–14]

Many changing cellular structures, due to disease or injury, have already been shown to affect ADC measurements. Specifically for white matter imaging, some have measured changes in DTI metrics with changing myelin content or myelin damage.[2,15–22]

Axon Diameter Measurements from Diffusion Weighted MRI

There are several methods for estimating axon diameter distributions and densities using MRI and most use PGSE with ADC(Δ) or q-space. One method, AxCaliber, uses a framework that combines composite hindered and restricted models of water diffusion (CHARMED) and PGSE measurements.[23] This method uses one fixed gradient direction and multiple diffusion times and gradient strengths to make the CHARMED model more sensitive to axon diameter.[8] It fits the MR signal to an equation which has components due to restricted diffusion, hindered diffusion, and later free diffusion.[24] Water in each axon size will experience restricted diffusion at different Δ. For example, water in an axon with a small diameter will experience restriction for much smaller Δ than water in a larger axon.[2] Thus by shortening Δ, smaller and smaller axons move from the restricted component to the hindered component allowing the inference of axon diameter of smaller and smaller axons.

The framework used in AxCaliber for dividing the models into different types of diffusion was based on another model, which describes bovine optic nerve tissue as a three-compartment system, (axons, glial cells, and extracellular space). Each compartment has its own diffusion coefficient, size, volume fraction, membrane permeability, and NMR relaxation times. It uses multiple Δs and gradient strengths in a pulse sequence similar to PGSE (stimulated echo) which allows for longer diffusion times and measures the mean axon diameter, but not the distribution.[25]

Another method, ActiveAx, extended and optimized these methods to determine the accuracy and precision with which this important new biomarker, axon diameter, can be estimated in live human subjects.[9] The work from this group combined a simplified version of CHARMED with high-angular-resolution diffusion imaging (HARDI) and a model with a single axon diameter.[9] It has been modified to be robust in the presence of orientation dispersion.[26] The same group has also combined two-shell HARDI with a three-compartment tissue model to create neurite orientation dispersion and density imaging (NODDI).[27] Table 1 summarizes the literature for some of the axon diameter measurements made with MRI. Diffusion times used ranged from 7 to 305 ms measuring diameters from 0.4–14 µm. Measuring similar restriction sizes in porous objects at room temperature would likely need longer imaging times because of the slower diffusion at the lower room temperature compared to body temperature.

Measuring axon diameter distributions with MRI, even with intact ex vivo brains, has advantages over traditional ex vivo histological techniques. Ex vivo histological techniques are cumbersome, require tissue sectioning and are subject to inaccuracies such as cell shrinkage.[9] With MRI, the brain remains intact and images can provide measurements over large regions of the brain. Because of the difficulties with ex vivo histological measurements of axon diameter distributions, the variation of fiber composition over the population and during development is largely unstudied.[9]

Although fixation can affect samples, studies have been done to compare ADC and other DTI metrics between in vivo and fixed ex vivo samples.[22,28–30] While

Table 1. A summary of some previous MRI measures of axon diameters. The measured diameters ranged from 0.4 to 14 µm using diffusion times ranging from 7 to 305 ms

Manuscript	Sample	Mean neuron diameters based on histology (µm)	Mean neuron diameters based on diffusion MRI (µm)	Diffusion time (ms)
Stanisz[25]	Bovine optic nerve	2–3	2.6	7–29
Assaf[23]	Excised rat brain tissue	Not measured	1–2 and 6–8	35–305
Assaf[8]	Porcine sciatic nerve	7.3	6.3	9.17–79.17
Assaf[8]	Porcine optic nerve	3.48	3.74	9.17–79.17
Barazany[24]	Rat corpus callosum	0–3	0.4–8	9.9–99.9
Alexander[9]	Fixed monkey brain	1–3	2–8	12.7–23.7
Alexander[9]	Human corpus callosum	2–6	6–14	15.7–85.3
Zhang[26]	Human corpus callosum	Not measured	6.8–11.7	15.7–85.3
Zhang[26]	Human centrum semiovale	Not measured	6.8–13.3	15.7–85.3

absolute values of ADC change, partially due to the temperature of the sample, fractional anisotropy is similar.[31] Thus ex vivo measurements of axon diameters on intact fixed brains can still offer important information.

Limits to the Ability to Measure Small Axon Diameters

The PGSE sequence requires, however, that Δ be large with respect to the restriction sizes in biological tissues, thus limiting the information that could be obtained from the measurements as will now be explained. The signal from a PGSE sequence is given by $\ln\left(S/S_0\right) = -\gamma^2 \delta^2 g^2 \left(\Delta - \delta/3\right) D = -bD$, where γ is the gyromagnetic ratio of the hydrogen nucleus, δ is the duration of the gradient pulse, and g is the amplitude of the gradient pulse. In order to measure the diffusion coefficient, the difference in signal with, S, and without, S_0, diffusion gradients has to be large enough compared to the noise. Thus a large $b = \gamma^2 \delta^2 g^2 \left(\Delta - \delta/3\right)$ value is needed. Given that small Δs are desired, and $\delta < \Delta$ for PGSE, the only remaining factor that can be increased is the gradient strength. With q-space imaging, the smallest displacements which can be probed depend on the largest q which can be used.[8] Again, to make a large q, large gradient strengths need to be used. Gradient coils are limited in power they can supply. Moreover, for small duration, large amplitude gradient pulses, there will be a large change in magnetic field experienced by the subject in a short amount of time. This induces an electric field in the subject, which could cause twitching of the skin, pain, or interference with the function of the heart or brain.[32]

Thus, in practice, it is difficult to make measurements at short diffusion times using the PGSE sequence. PGSE signals from water molecules in small axons do not change with diffusion time in the typical range used. Thus methods to determine axon diameter from these PGSE measurements are insensitive to these small axons. Shortening Δ would allow the inference of restriction sizes, for example rodent sized axon diameters, and surface-to-volume ratios in samples. However, such measurements presently cannot be done with PGSE as described above.[32,33]

Oscillating Gradient Spin Echo Sequences

In 1969, an oscillating gradient spin echo (OGSE) sequence was proposed to make measurements at short diffusion times,[34] see Figure 2. In this sequence, the trapezoidal gradient pulses of the PGSE sequence are replaced with sinusoidally varying gradient pulses. Each period of the sine wave acts as a diffusion weighting so that the magnetic moments are dephased by the first lobe of the sine wave and rephased by the second lobe. These sine waves are repeated multiple times so that sufficient diffusion weighting can be obtained. The first measurements were made of surface-to-volume ratios from packed beads in water[33] and in vegetables.[36]

However, only in the case of unrestricted Brownian motion can these multiple diffusion-weighting periods be considered independent.[37,38] For this reason, the signal attenuation should be described in terms of a frequency spectrum rather than simply a scalar value (Δ). More complicated gradient modulations that selectively sample a narrow frequency domain of the diffusion spectrum have been proposed.[39] These provide a straightforward means of characterizing the diffusion spectrum, but are difficult to implement accurately.[35] Thus double-sine- and apodized cosine-modulated gradient waveforms, which are modified forms of OGSE, have been used and are still termed OGSE sequences.[35] In this so-called temporal diffusion spectroscopy, the effective diffusion times are changed by varying diffusion gradient frequencies, and thus a spectrum of diffusion rates, which describe the biological tissue microenvironment, can be measured. These measurements are different from q-space imaging where the propagator is usually defined at a given long diffusion time and has spatial and directional dependences over a large range of q-space.[5,40] The contrast between
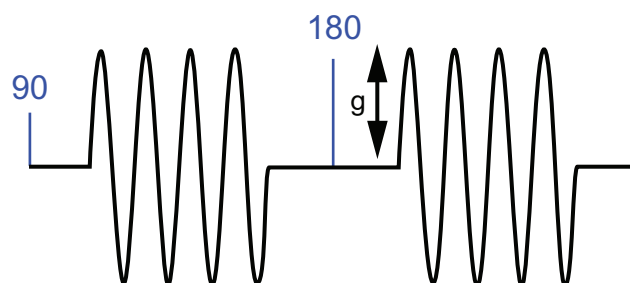
Figure 2. Oscillating gradient spin echo (OGSE) sequence. The basic OGSE sequence consists of two RF pulses, shown in blue, and two sinusoidally oscillating gradient pulses, shown in black. In theory, the higher the frequency of the gradient pulses, the smaller the structures that can be probed. More complicated OGSE sequences which provide a straightforward means of characterizing the diffusion spectrum, change the form of the sine wave gradient pulses to apodized cosine or double sine waves.[35]

tissues might be greater at a discrete, moderately high frequency than at low frequencies, as suggested by theoretical consideration of simple geometries and preliminary studies in tumors[41] and rat brain.[42]

Using OGSE sequences might improve axon measurements. As Alexander notes: "More significant improvements may come from replacing the standard PGSE sequence with other diffusion-sensitive sequences such as oscillating gradient … experiments, which may be more sensitive to microstructural parameters. … Combination of the experiment design with these other pulse sequences should allow the a priori range of axon diameters to extend to include smaller diameters. This should provide protocols with sensitivity to wider ranges and provide more discriminative axon diameter indices."[9] This same group performed experiments with optimized gradient waveforms (GEN) and were able to make axons with smaller radii more distinguishable with GEN than with PGSE.[43,44] They still suggest that oscillating waveforms would provide valuable information for in vivo studies.[43] Developing DTI techniques to visualize better smaller fibers is considered an active area of research[45] and creating new techniques using short diffusion times will cause water in the larger fibers to become less restricted allowing for easier visualization of the restricted diffusion of water in the smaller fibers.

OGSE and Axon Diameter Measurements

Extending the measurements made with OGSE from studying the variation of ADC with diffusion time or frequency to create a method which uses this variation to infer restriction sizes using the shortest possible diffusion times could allow for the probing of smaller axon diameters. In theory, this method overcomes problems with high gradient strengths necessary in current MR diffusion methods (PGSE and q-space) to allow smaller restriction sizes to be distinguished.[35] The OGSE and PGSE methods could be used together to distinguish a large range of restriction sizes from very small (OGSE) to fairly large (PGSE). Combining the two methods might allow for a more complete understanding of the geometry of the sample.

Author Contributions

Conceived and designed the concept: MM. Wrote the first draft of the manuscript: MM. Agree with manuscript conclusions: MM. Made critical revisions: MM. The author reviewed and approved of the final manuscript.

Competing Interests

Author(s) disclose no potential conflicts of interest.

Disclosures and Ethics

As a requirement of publication the author has provided signed confirmation of compliance with ethical and legal obligations including but not limited to compliance with ICMJE authorship and competing interests guidelines, that the article is neither under consideration for publication nor published elsewhere, of their compliance with legal and ethical guidelines concerning human and animal research participants (if applicable), and that permission has been obtained for reproduction of any copyrighted material. This article was subject to blind, independent, expert peer review. The reviewers reported no competing interests. Provenance: the author was invited to submit this paper.

References

1. Einstein A. Über die von der molekularkinetischen Theorie der Wärme geforderte Bewegung von in ruhenden Flüssigkeiten suspendierten Teilchen. *Ann Physik.* 1905;4:549–60.
2. Jones DK, editor. *Diffusion Theory, Methods and Application.* Oxford; 2011.
3. Price WS. Pulsed-field gradient nuclear magnetic resonance as a tool for studying translational diffusion part 1: basic theory. *Concept Magn Reson.* 1997:9(5):299–336.
4. Stejskal EO, Tanner JE. Spin diffusion measurements: Spin echoes in the presence of a time-dependent field gradient. *J Chem Phys.* 1965;42(1):288–92.
5. Callaghan PT, Eccles CD, Xia Y. NMR Microscopy of Dynamic Displacements—k-space and q-space Imaging. *J Phys E Sci Instrum.* 1988;21:820–2.
6. Basser PJ. Inferring microstructural features and the physiological state of tissues from diffusion-weighted images. *NMR Biomed.* 1995;8(7–8):333–44.
7. Cohen Y, Assaf Y. High b-value q-space analyzed diffusion-weighted MRS and MRI in neuronal tissue—a technical review. *NMR Biomed.* 2002; 15(7–8):516–542.
8. Assaf Y, Blumenfeld-Katzir T, Yovel Y, Basser PJ. AxCaliber: a method for measuring axon diameter distribution from diffusion MRI. *Magn Reson Med.* 2008;59(6):1347–54.
9. Alexander DC, Hubbard PL, Hall MG, et al. Orientationally invariant indices of axon diameter and density from diffusion MRI. *Neuroimage.* 2010;52(4):1374–89.
10. Basser PJ, Jones DK. Diffusion-tensor MRI: theory, experimental design and data analysis—a technical review. *NMR Biomed.* 2002;15(7–8):456–67.
11. Le Bihan D, Breton E, Lallemand D, Grenier P, Cabanis E, Lavaljeantet M. MR imaging of intravoxel incoherent motions: application to diffusion and perfusion in neurologic disorders. *Radiology.* 1986;161(2):401–7.

12. Turner R, Le Bihan D, Chesnick AS. Echo-planar imaging of diffusion and perfusion. *Magn Reson Med*. 1991;19(2):247–53.

13. Bammer R. Basic principles of diffusion-weighted imaging. *Eur J Radiol*. 2003;45(3):169–84.

14. Le Bihan D. Molecular diffusion nuclear magnetic resonance imaging. *Magn Reson Q*. 1991;7(1):1–30.

15. Odrobina EE, Lam TYJ, Pun T, Midha R, Stanisz GJ. MR properties of excised neural tissue following experimentally induced demyelination. *NMR Biomed*. 2005;18(5):277–84.

16. Underhill HR, Rostomily RC, Mikheev AM, Yuan C, Yarnykh VL. Fast bound pool fraction imaging of the in vivo rat brain: association with myelin content and validation in the C6 glioma model. *Neuroimage*. 2011;54(3): 2052–65.

17. Song SK, Yoshino J, Le TQ, et al. Demyelination increases radial diffusivity in corpus callosum of mouse brain. *Neuroimage*. 2005;26(1):132–40.

18. Budde MD, Xie M, Cross AH, Song SK. Axial diffusivity is the primary correlate of axonal injury in the experimental autoimmune encephalomyelitis spinal cord: a quantitative pixelwise analysis. *J Neurosci*. 2009;29(9): 2805–13.

19. Xie M, Tobin JE, Budde MD, et al. Rostrocaudal analysis of corpus callosum demyelination and axon damage across disease stages refines diffusion tensor imaging correlations with pathological features. *J Neuropathol Exp Neurol*. 2010;69(7):704–16.

20. Sun SW, Liang HF, Trinkaus K, Cross AH, Armstrong RC, Song SK. Noninvasive detection of cuprizone induced axonal damage and demyelination in the mouse corpus callosum. *Magn Reson Med*. 2006;55(2):302–8.

21. Beaulieu C. The basis of anisotropic water diffusion in the nervous system—a technical review. *NMR Biomed*. 2002;15(7–8):435–55.

22. Song SK, Sun SW, Ramsbottom MJ, Chang C, Russell J, Cross AH. Dysmyelination revealed through MRI as increased radial (but unchanged axial) diffusion of water. *Neuroimage*. 2002;17(3):1429–36.

23. Assaf Y, Cohen Y. Non-mono-exponential attenuation of water and N-acetyl aspartate signals due to diffusion in brain tissue. *J Magn Reson*. 1998;131(1): 69–85.

24. Barazany F, Basser PJ, Assaf Y. In vivo measurement of axon diameter distribution in the corpus callosum of rat brain. *Brain*. 2009;132(5):1210–20.

25. Stanisz GJ, Szafer A, Wright GA, Henkelman RM. An analytical model of restricted diffusion in bovine optic nerve. *Magn Reson Med*. 1997;37(1): 103–11.

26. Zhang H, Hubbard PL, Parker GJM, Alexander DC. Axon diameter mapping in the presence of orientation dispersion with diffusion MRI. *Neuroimage*. 2011;56(3):1301–15.

27. Zhang H, Schneider T, Wheeler-Kinshot CA, Alexander DC. NODDI: Practical in vivo neurite orientation dispersion and density imaging of the human brain. *Neuroimage*. 2012;61(4):1000–16.

28. Schmierer K, Wheeler-Kingshot CAM, Tozer DJ, et al. Quantitative magnetic resonance of postmortem multiple sclerosis brain before and after fixation. *Magn Reson Med*. 2008;59(2):268–77.

29. Concha L, Livy DJ, Beaulieu C, Wheatley BM, Gross DW. In vivo diffusion tensor imaging and histopathology of the fimbria-fornix in temporal lobe epilepsy. *J Neurosci*. 2010;30(3):996–1002.

30. Douaud G, Jbabdi S, Behrens TEJ, et al. DTI measures in crossing-fibre areas: increased diffusion anisotropy reveals early white matter alteration in MCI and mild Alzheimer's disease. *Neuroimage*. 2011;55(3):880–90.

31. Sun SW, Neil JJ, Liang HF, et al. Formalin fixation alters water diffusion coefficient magnitude but not anisotropy in infarcted brain. *Magn Reson Med*. 2005;53(6):1447–51.

32. Schaefer DJ, Bourland JD, Nyenhuis JA. Review of patient safety in time-varying gradient fields. *J Magn Reson Imaging*. 2000;12(1):20–9.

33. Schachter M, Does MD, Anderson AW, Gore JC. Measurements of restricted diffusion using an oscillating gradient spin echo sequence. *J Magn Reson*. 2000;147(2):233–7.

34. Gross B, Kosfeld R. Anwendung der spin-echo-methode der messung der selbstdiffusion. *Messtechnik*. 1969;77:171–7.

35. Does MD, Parsons EC, Gore JC. Oscillating gradient measurements of water diffusion in normal and globally ischemic rat brain. *Magn Reson Med*. 2003;49(2):206–15.

36. Gore JC, Anderson AW, Does MD, et al. The relationship of problems in biomedical MRI to the study of porous media. *Magn Reson Imag*. 2001;19(): 295–300.

37. Stepisnik J. Analysis of self-diffusion measurements by density matrix calculation. *Physica*. 1981;104B:350–64.

38. Stepisnik J. Measuring and imaging of flow by NMR. *Prog NMR Spec*. 1985;17:187–209.

39. Callaghan PT, Stepisnik J. Frequency-domain analysis of spin motion using modulated-gradient NMR. *J Magn Reson*. 1995;117():232–7.

40. Mori S, van Zijl PCM. Fiber tracking: principles and strategies—a technical review. *NMR in Biomedicine*. 2002;15(7–8):468–80.

41. Gore JC, Xu J, Colvin DC, Yankeelov TE, Parsons EC, Does MD. Characterization of tissue structure at varying length scales using temporal diffusion spectroscopy. *NMR Biomed*. 2010;23(7):745–56.

42. Kershaw J, Leuze C, Obata T, Kanno I, Aoki I. Changes to the fractional anisotropy and mean diffusivity of in vivo rat brain measured at short effective diffusion-times. *Proc Intl Soc Mag Reson Med*. 2011;19:409.

43. Siow B, Drobnjak I, Chatterjee A, Lythgoe MF, Alexander DC. Estimation of pore size in a microstructure phantom using the optimized gradient waveform diffusion weighted NMR sequence. *J Magn Reson*. 2012;214(1): 51–60.

44. Drobnjack I, Siow B, Alexander DC. Optimizing gradient waveforms for microstructure sensitivity in diffusion-weighted MR. *J Magn Reson*. 2010;206(1):41–51.

45. Rane S, Duong TQ. Comparison of *in vivo* and *ex vivo* diffusion tensor imaging in rhesus macaques at short and long diffusion times. *Open Neuroimag J*. 2011;5:172–8.